2012 IEEE International Conference on Robotics and Automation
RiverCentre, Saint Paul, Minnesota, USA
May 14-18, 2012

Soft Tissue Force Control Using Active Observers and Viscoelastic Interaction Model

Pedro Moreira, Chao Liu, Nabil Zemiti and Philippe Poignet

Abstract— **Controlling the interaction between the robot and living soft tissues has became an important issue as the number of robots inside the operating room increases. Many research works have been done in order to control this interaction. Nowadays, researches are running in force control for helping surgeons in medical procedures such as motion compensation in beating heart surgeries and tele-operation systems with haptic feedback. The viscoelasticity property of the interaction between organ tissue and robotic instrument further complicates the force control design which is much easier in other applications by assuming the interaction model to be elastic (industry, stiff object manipulation, etc.). In order to increase the performance of a model based force control, this work presents a force control scheme using Active Observer (AOB) based on a viscoelastic interaction model. The control scheme has shown to be stable through theoretical analysis and its performance was evaluated and compared with a control scheme based on a classical elastic model through experiments, showing that a more realistic model can increases the performance of the force control.**

I. INTRODUCTION

Understanding the interaction between medical tools and living tissues has become a very important aspect as the use of robot in medical application increases. Medical robots can work together with surgeons helping to create a less invasive and more precise surgery. The need of better technologies for surgery is illustrated by the great number of researches running all over the world on how robots can help on procedures such as interventional radiology and microsurgery.

In all these procedures, the robot or the medical tool guided by the robot needs to get in contact with several types of soft tissues. In order to avoid tissue damage, the contact force and the tissue deformation should be precisely controlled.

One of the first works applying force control to medical robots is presented in [1], where the force feedback was used to provide safety, tactile capabilities and improve the man/machine interface. More recently, force control has been studied to implement tele-operational systems with haptic feedback [16], and also to reject disturbances forces caused by physiological motions [6]. In this last application, the use of classical force controllers may not achieve a good disturbance rejection, mainly because of its bandwidth limitation [5]. Hence, increase the performance of force controllers in contact with soft tissue can significantly improve the use of robots in medical procedures.

Some force controllers specially designed for medical applications in the literature simply do not use any tissue model in its design, such as the work presented in [3] for beating heart motion compensation, which proposes a force feedback controller with a feed-forward term composed by the estimated tissue velocity and acceleration. For the same purpose, a control loop based on Iterative Learning Control (ILC) is implemented in addition to a conventional inner force feedback control loop in [5].

In [4] an adaptive state feedback force control using Active Observer (AOB) is proposed considering the soft tissue as an elastic environment. The AOB is a stochastic observer used to estimate system states and an extra state is added to compensate for modeling errors and system disturbances. This control scheme has been implemented in tele-operational systems with haptic feedback and also implemented for physiological motion compensation. Motion compensation experiments using beating heart motion are presented in [6] and the conclusion reached by the authors is that the controller cannot be considered without further improvements.

The force control scheme presented in [4] and classical force controllers use an elastic spring as interaction model. Unfortunately, biomechanics characteristics of tissues are nonlinear, inhomogeneous and anisotropic [7], which makes this interaction modeling between the tool and the tissue a complicated task. It is clear that purely elastic models cannot describe accurately the interaction between the robot and the tissue, specially when fast movements are involved, once the viscous characteristic of the tissue has a strong influence. Therefore, it is necessary to introduce more realistic model in order to increase the bandwidth and also the robustness of the control scheme against parameters mismatch.

A great number of research efforts dealing with robots in contact with viscoelastic surfaces are running on humanoid robots, such as in [2] where a Hunt-Crossley contact model is used to control a robot that moves in free-space and then undergoes a collision with a viscoelastic environment. Conversely, in medical applications, the main works using more complex models focus on position control and needle insertion simulation [8], [9], [10], [11], [12].

The most widespread modeling method in the literature is the Finite Element Method (FEM) and it is used mostly for tissue simulation. FEM models can use either a linear relationship between stress and strain [13] or a nonlinear relationship [14]. Models based on this technique have a

This work was granted by ANR Contint USComp project

Pedro Moreira, Chao Liu, Nabil Zemiti and Philippe Poignet are with Laboratoire d'Informatique, de Robotique et de Microelectronique de Montpellier, Université Montpellier 2, Montpellier, France. pedro.moreira@lirmm.fr, liu@lirmm.fr, zemiti@lirmm.fr, poignet@lirmm.fr

good accuracy, but they are numerically time-consuming, specially for real-time applications. In [12] a polynomial function of second order is proposed to model the interaction between the needle and tissue in pre-puncture. A viscoelastic model based on fractional derivative is presented in [11]. The model has a good accuracy, specially when relaxation phenomenon is presented. The problem with this method are the computation time and the estimation processes for all parameters. A soft tissue model devoted to position control in needle insertion applications is proposed in [8] and consists in a Kelvin-Voigt model. In [10], a dynamic force model is presented, where the force is modeled using a nonlinear model.

In this work we aim to identify a more realistic and suitable viscoelastic model to be inserted in a force control scheme. The model is identified through experimental evaluations which should be both accurate enough to achieve the force control task and computationally efficient for real-time implementations. The force control scheme developed is a space state feedback using AOB. This control scheme possesses flexibility and has the possibility of being used in two important applications: motion compensation and tele-operation with haptic feedback.

The control scheme stability is analyzed theoretically so as its robustness under parameters mismatch. An experimental comparison between the force control designed using a viscoelastic model and the same controller using an elastic model were conducted to show that controllers with faster time response can be designed using a more realistic model, having at the same time a good robustness against parameters mismatch.

II. Soft Tissue Interaction Model

The objective of this section is to identify a soft tissue interaction model to be used in a real time force control. The compromise between accuracy and complexity is used as a criteria to eliminate some complex models, such as FEM models, fractional models and higher order models, due to their heavy computation and difficulties in estimating the models parameters. Therefore, three classical viscoelastic models and the purely elastic model were identified as good candidate models (Fig. 1). The purely elastic model is the simplest one, and the environment is modeled by a spring. The interaction force is described as:

$$F(t) = kx(t) \tag{1}$$

where $x(t)$ denotes position deformation, k represents the spring stiffness constant. The Maxwell model is composed of a spring and a damper in series and the interaction force F is described as:

$$F(t) = k\frac{dx(t)}{dt} - \alpha\frac{dF(t)}{dt} \tag{2}$$

where $\alpha = \frac{b}{k}$ and b is the damping factor. The Kelvin Voigt model is composed of a spring and a damper in parallel and the interaction force F is described as:

$$F(t) = b\frac{dx(t)}{dt} + kx(t) \tag{3}$$

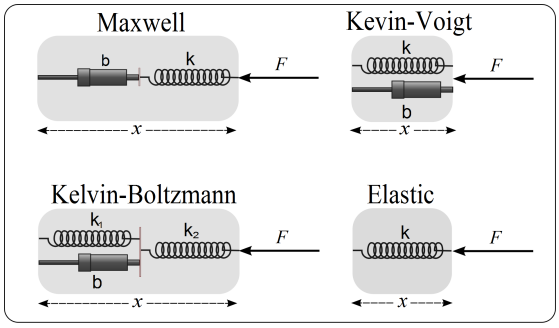

Fig. 1. Classical viscoelastic models and purely elastic model

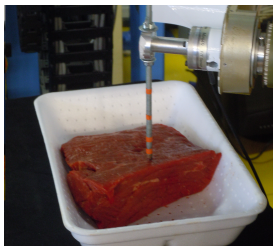

Fig. 2. Piece of beef used as specimen in the experiments

The Kelvin Boltzmann model combines the Kelvin Voigt model with a spring in series and the interaction force F is described as:

$$F(t) = \beta x(t) + \alpha\dot{x}(t) - \gamma\dot{F}(t), \tag{4}$$

where $\alpha = b\frac{k_2}{k_1+k_2}$, $\beta = \frac{k_1k_2}{k_1+k_2}$, $\gamma = \frac{b}{k_1+k_2}$.

Then, *in vitro* experimental studies have been conducted to evaluate the performance of these possible models and the one which fits best to our control task requirements was chosen to be used in the force control design.

A. Experiments

Different types of experiments can be performed in order to identify soft tissue characteristics. The two most common are relaxation and creep tests [7]. In this work, to identify the most suitable model, *in vitro* relaxations tests were performed. The test consists in performing a position step input on the soft tissue and measuring the exerted force.

A piece of beef was used as specimen in these experiments (Fig.2). It is clear that this kind of specimen used in *in vitro* experiments has limitations. The biomechanical characteristics of an *in vitro* specimen differ from the characteristics of living soft tissues. This fact can be explained mainly by the absence of vascularisation. Nevertheless, the use of *in vitro* specimen is very common and can provide results close to the one obtained with living tissues [7].

All tests were performed using the D2M2 robot. It has five degrees of freedom with direct drive technology providing fast dynamics and low friction. The first joint is prismatic and the other four are revolute joints. A force sensor (ATI Mini40) is attached to the end effector. The tool in contact with the soft tissue is a metallic cylinder with a diameter of $6mm$. More information about the robot can be read in [16].

TABLE I

ESTIMATED PARAMETERS FOR EACH MODEL

Model	Parameter	Value	Stand. Dev.
Elastic	k	205.8	0.337%
Maxwell	α	0.001	0.8442%
	b	486.5	4.21%
Kelvin-Voigt	b	17.4891	3.50%
	k	203.5	0.31%
Kelvin Boltzmann	α	43.6069	2.72%
	β	200.0	0.30%
	γ	0.07	3.99%

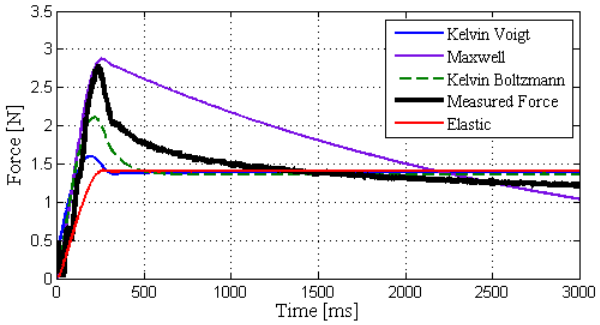

Fig. 3. Relaxation Tests performed in a *in vitro* specimen.

The information of position input and force output measured were collected and used to estimate the parameters of each model. For this estimation an off-line least square algorithm was used. Using the identified parameters, off-line simulations were performed applying the input information collected on experiments in each estimated model equation. The output for each model is then compared with the measured force to analyze its accuracy.

B. Results

Several relaxation tests were performed on different points of the specimen surface with input values varying from $9mm$ to $15mm$. In each test, the parameters of the four models were estimated by the off-line least square algorithm. For the seek of clarity, one relaxation test with position input defined as $10mm$ is presented. The estimated parameters and its standard deviation are shown in Table I. Each model were simulated and the force outputs can be seen in Fig. 3.

As expected, the linear model reaches approximately the final value, but it does not follow the tissue dynamics. The Kelvin-Boltzmann model and the Kelvin-Voigt model had the most realistic response, reaching approximately the final value and following the tissue dynamic, but the Kelvin-Boltzmann model gives the lowest error. The root mean square error (RMSE) in $[N]$ of each estimated force are:

Elastic = 0.29, Kelvin Voigt = 0.26
Maxwell = 0.44, Kelvin Boltzmann = 0.19

The values of root mean square error confirm the analysis made by graphic inspection, which is the Kelvin Boltzmann model gave the lowest error among the four models.

In order to perform a cross validation, the mean values of the parameters estimated in ten different relaxation tests were used. The mean values can be seen in table II.

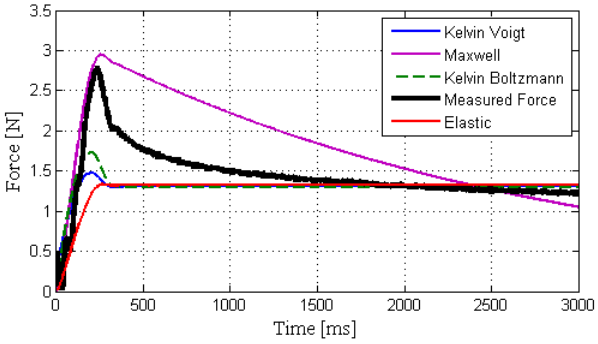

Fig. 4. Cross validation simulations

TABLE II

MEAN VALUES OF ESTIMATED PARAMETERS

Kelvin Boltzmann	$\alpha = 27.2$, $\beta = 190.2$, $\gamma = 0.0345$
Kelvin Voigt	$k = 192.7$, $b = 14.7$
Maxwell	$k = 596.0$, $\alpha = 0.79$
Elastic	$k = 194.0$

The simulations results were again compared with the measured force (Fig.4). The root mean square error for each model are:

Elastic = 0.30, Kelvin Voigt = 0.28
Maxwell = 0.47, Kelvin Boltzmann = 0.25

Again, the Kelvin Boltzmann model gave the lowest root mean square error.

According to the performed tests, among the viscoelastic models, the Kelvin-Boltzmann is the one that presents the most realistic results with a dynamic response closer to the real one. This can be explained by the presence of the force derivative, which brings more information about the transient period. In the Kelvin-Boltzmann equation, the parameter β is obtained as a combination of the two springs coefficients, and is related to tissue's stiffness. The parameters α and γ are related to the tissue's viscosity and are responsible for the transient accuracy of the model.

For the next, the Kelvin-Boltzmann model was chosen to be inserted in the force control scheme.

III. FORCE CONTROL USING ACTIVE OBSERVERS

A. Dynamic Equation

The dynamic equation of the robot in the Cartesian space in contact with an environment is given by [18]:

$$M_x(q)\ddot{q} + v_x(\dot{q}, q) + g_x(q) = F_t - F_e \qquad (5)$$

where M_x is the operational space mass matrix, v_x is the vector of Coriolis and centripetal forces, g_x is the gravity term, X is the Cartesian position, q is the robot joint position, F_t is the Cartesian commanded force and F_e is the external interaction force.

In order to achieve the desired decoupled system

$$f^* = \ddot{X} \tag{6}$$

the commanded force is computed as

$$F_t = \hat{F}_e + \hat{M}_x(q) f^* + \hat{v}_x(\dot{q}, q) + \hat{g}_x(q) \tag{7}$$

where $\hat{F}_e$, $\hat{M}_x$, $\hat{v}_x$ and $\hat{g}_x$ are respectively the estimation of F_e, M_x, v_x and g_x. The acceleration f^* is an input signal and the system given by (6) is a unity mass system along each Cartesian dimension. After adding a velocity loop with a gain k_v, the linearized model is highlighted in Fig. 5, where u is the control signal and F is the force output.

B. State space equation for the linearized system

Using the Kelvin-Boltzmann model equation, the transfer function of the linearized system is given in the Cartesian as

$$\frac{F}{u} = \frac{\alpha s + \beta}{s^3 + (k_v + 1/\gamma)s^2 + k_v/\gamma s} \tag{8}$$

where s is the Laplace operator and α, β and γ are model parameters identified previously. The space state form is obtained by the observer canonical form [19]:

$$\begin{bmatrix} \dot{x_1} \\ \dot{x_2} \\ \dot{x_3} \end{bmatrix} = \begin{bmatrix} -k_v - 1/\gamma & 1 & 0 \\ -k_v/\gamma & 0 & 1 \\ 0 & 0 & 0 \end{bmatrix} \begin{bmatrix} x_1 \\ x_2 \\ x_3 \end{bmatrix} + \begin{bmatrix} 0 \\ \alpha/\gamma \\ \beta/\gamma \end{bmatrix} u(t) \tag{9}$$

$$y(t) = \begin{bmatrix} 1 & 0 & 0 \end{bmatrix} \begin{bmatrix} x_1 \\ x_2 \\ x_3 \end{bmatrix} \tag{10}$$

where, the state x_1 is the force, the state x_2 is a combination of the derivative of the force and the input, and the state x_3 is a combination of the second derivative of the force and the derivative of the input. The space state systems is discretized to be used to design the AOB and the state feedback gain.

C. Active Observer Based Controller

Differently from classical force control design, where the design is usually blind to the noises present in the whole system, the AOB provides a methodology to achieve model-reference adaptive control through extra states and stochastic design. Based on a desired closed loop system, an extra state p_k is added to compensate for disturbances and unmodeled terms through the state feedback.

The discrete system is obtained from (9) and (10) and is given by:

$$x_{r,k} = \Phi_r x_{r,k-1} + \Gamma_r u_{k-1} + \zeta \tag{11}$$

$$y_k = C_r x_{r,k} + \eta \tag{12}$$

where Φ_r and Γ_r are the system and input discrete matrices, C_r is the output matrix and ζ and η are Gaussian random variables associated to the system and to the measures, respectively. The control signal u is defined as:

$$u_k = r_k - \begin{bmatrix} L_r & 1 \end{bmatrix} \begin{bmatrix} \hat{x}_{r,k} \\ \hat{p}_k \end{bmatrix} \tag{13}$$

where $\hat{x}_{r,k}$ are the estimated system states, p_k is the active state, r_k is the input reference and L_r is the feedback gain used to tune the system response in closed loop. The overall control scheme is depicted in Fig. 5. Since the plant has an integrator, only a gain L_1 multiplying the desired force is needed to eliminate the steady state error [19].

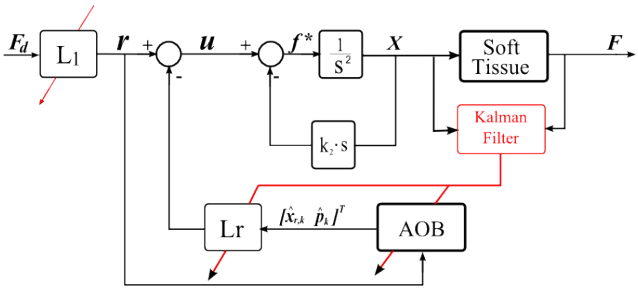

Fig. 5. Overall force control scheme using Active Observer

The state estimation carried out by the AOB is given by:

$$\begin{bmatrix} \hat{x}_{r,k} \\ \hat{p}_k \end{bmatrix} = \begin{bmatrix} \Phi_r - \Gamma_r L_r & 0 \\ 0 & 1 \end{bmatrix} \begin{bmatrix} \hat{x}_{r,k-1} \\ \hat{p}_{k-1} \end{bmatrix} + \\ + \begin{bmatrix} \Gamma_r \\ 0 \end{bmatrix} r_{k-1} + K_k(y_k - \hat{y}_k) \tag{14}$$

where the estimated output $\hat{y}_k$ is

$$\hat{y}_k = C_a \left(\begin{bmatrix} \Phi_r - \Gamma_r L_r & 0 \\ 0 & 1 \end{bmatrix} \begin{bmatrix} \hat{x}_{r,k-1} \\ \hat{p}_{k-1} \end{bmatrix} + \begin{bmatrix} \Gamma_r \\ 0 \end{bmatrix} r_{k-1} \right) \tag{15}$$

and $C_a = \begin{bmatrix} C_r & 0 \end{bmatrix}$.

The matrix K_k is the Kalman gain and is related to the uncertainty of each state. The Kalman gain is calculated by:

$$K_k = P_{1k} C_a^T (C_a P_{1k} C_a^T + R_k)^{-1} \tag{16}$$

$$P_{1k} = \Phi_n P_{k-1} \Phi_n^T + Q_k \tag{17}$$

$$P_k = P_{1k} - K_k C_a P_{1k} \tag{18}$$

The matrix Φ_n is called the augmented open loop matrix and has the form:

$$\Phi_n = \begin{bmatrix} \Phi_r & L_r \\ 0 & 1 \end{bmatrix} \tag{19}$$

The matrices Q_k and R_k are respectively the system noise and the measurement noise matrix, Q_k has the form:

$$Q_k = \begin{bmatrix} Q_x & 0 \\ 0 & Q_p \end{bmatrix}$$

where, Q_p is the system noise in respect to the system states and Q_x is the system noise in respect to the active state. The estimation strategy depends on the relation between the Q_k and R_k values [4]. If the model accuracy is very good compared to measurement accuracy ($Q_k << R_k$), a model-based approach is followed with low Kalman gain values. On the other hand, if the measurement is more accurate ($Q_k >> R_k$), a sensor based approach is followed with high Kalman gain values [16].

D. Stability and Robustness

Stability: stability analysis is very important in control systems design. The stability analysis is made through the phase and gain margins of the loop transfer function (LTF) [20], which is the product of the transfer functions of forward and feedback loops. The LTF of the overall system without model errors is described by

$$\begin{bmatrix} \hat{x}_k \\ e_k \end{bmatrix} = \begin{bmatrix} \Phi - (I - K_k C)\Gamma L & K_k C\Phi \\ (I - K_k C)\Gamma L & (I - K_k C)\Phi \end{bmatrix} \cdot \begin{bmatrix} \hat{x}_{k-1} \\ e_{k-1} \end{bmatrix} + \begin{bmatrix} K_k C\Gamma \\ (I - K_k C)\Gamma \end{bmatrix} u_{k-1}$$

$$Y = \begin{bmatrix} L & 0 \end{bmatrix} \cdot \begin{bmatrix} \hat{x}_k \\ e_k \end{bmatrix} \quad (20)$$

where $\hat{x}_k = \begin{bmatrix} \hat{x}_{r,k} & \hat{p}_k \end{bmatrix}^T$ and $e_k = x_k - \hat{x}_k$. Then, knowing the LTF representation in state space it is straightforward to compute Nyquist/Bode plots and the corresponding phase and gain margins. Considering the model identified in section II, $Q_x = 10^{-11}$, $Q_p = 10^{-6}$, $R_k = 0.05$ and designing a controller with a rise time $\tau_r = 0.5s$, we obtain as phase and gain margins

$$Pm = 39.17^\circ \text{ and } Gm = 3.98dB.$$

Robustness: this analysis can be also used to determine the stability under parameters mismatch. The system LTF with model errors is given by

$$\begin{bmatrix} \hat{x}_k \\ e_k \end{bmatrix} = \begin{bmatrix} \Phi_n - \Gamma_n L + K_k C(\Delta\Phi + \Gamma_n L) & K_k C\Phi \\ (I - K_k C)(\Delta\Phi + \Gamma_n L) & (I - K_k C)\Phi \end{bmatrix} \cdot \begin{bmatrix} \hat{x}_{k-1} \\ e_{k-1} \end{bmatrix} + \begin{bmatrix} K_k C\Gamma \\ (I - K_k C)\Gamma \end{bmatrix} u_{k-1}$$

$$Y = \begin{bmatrix} L & 0 \end{bmatrix} \cdot \begin{bmatrix} \hat{x}_k \\ e_k \end{bmatrix} \quad (21)$$

where, Φ is real value of the system matrix and it is given by $\Phi = \Phi_n + \Delta\Phi$, the same is applied to Γ.

In the Kelvin Boltzmann case, this mismatch can occurs on three parameters. To study the influence of the mismatch in each parameter, an error was added in one at a time and also in the three parameters at the same time. The error was add as $\theta = \theta_n + \Delta\theta$, where θ is the parameter under mismatch and θ_n is its nominal value used to design the AOB. The graphic of phase margin and gain margin versus the parameter mismatch can be seen in Fig.6.

The phase margin analysis shows that, for this specific case, the system has proved to be stable with mismatches up to 150% ($Pm = 0$), which is sufficient for our application. It is possible to observe that for all cases the system becomes unstable as the mismatch becomes bigger. Anyhow, looking to the graph one can conclude that the mismatches in α and γ change the phase and gain margins, but do not create unstable systems. On the other hand, the stiffness parameter β can be pointed as the critical parameter, unstabilizing the system with a smaller mismatch than the others parameters. It is also the one that mostly determine the phase margin when all parameters have errors. To cope with this mismatch problem an on-line estimation of the stiffness parameter should be performed.

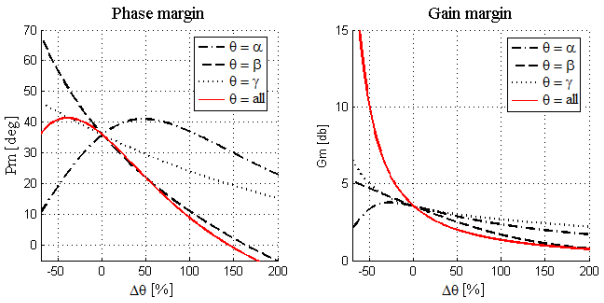

Fig. 6. Phase margin and gain margin considering parameters mismatch

E. On-line estimation

In practical applications, the model parameters may vary along the procedure due the complexity of tissues and its non-linearity. For that reason, an on-line updating of parameters is desirable and can increases the relative stability of the system.

In theory the three parameters can be estimated in the Kelvin Boltzmann model, but in practice one can only guarantee convergence in the estimation of parameters when sufficient excited. In addition, according to the results given in the previous subsection, the mismatch in the parameter β is the one that most influences the stability of the system. For these reasons we decided to perform an on-line estimation only in the parameter β.

The parameters α and γ were estimated off-line and will not be updated. The off-line values of these parameters were defined using the mean values of ten relaxation experiments. Therefore, the Kelvin Boltzmann model is written as

$$f(t) = -0.0345\frac{df(t)}{dt} + 27.3\frac{dx(t)}{dt} + \beta_k x(t)$$

where β_k is the stiffness parameter and it is estimated on-line by a Kalman Filter. As depicted in Fig.5, the estimative of β is used to update the AOB matrices and the feedback gain matrix.

IV. Experimental Results

The experiments were performed using the D2M2 robot on the same specimen used in section II. The experiment consists in a force control with the robot in contact with the tissue surface. As shown in Fig.5, the desired force is the system input and the output is the measured force.

In the experiments, $R = 0.05$, $Q_x = 10^{-11}$ and $Q_p = 10^{-6}$ were used. With these values the AOB is set to be model-based.

The feedback gain L_r was calculated using the Ackermann's formula in order to allocate the poles of the closed loop system to avoid overshoot.

Due to the closed loop characteristic of the AOB, it is not possible to allocate one pole to cancel the zero in the closed loop transfer function. Otherwise, the system will have the order reduced and the observability matrix will lose rank, consequently the system will lose observability. Then,

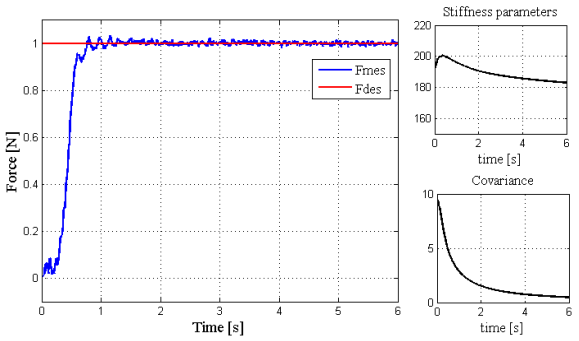

Fig. 7. Measured force in surface contact experiment

a trade-off between time response and overshoot appears in the control design.

A. Experimental evaluation

A first experiment with a $1N$ step input was performed to evaluate the system performance. A step force input was chosen to evaluate the controller under fast input transitions.

The desired force and the measured force can be seen in Fig. 7. In the same figure it is possible to see the evolution of the estimated parameter, converging to the value of $185N/m$. Experiments with different initial conditions and different desired closed loop poles are shown in the following.

B. Kelvin Boltzmann model vs. elastic model

In order to analyze the improvement of using a more realistic model in the force control scheme, an experimental comparison was performed between the force control using the Kelvin-Boltzmann model and the same type of controller designed with a traditional elastic model, which is the most used model in the literature so far.

The elastic AOB parameters, such as the system and measurement noise matrices and the desired closed loop poles were set with the same values used in the last section for the Kelvin-Boltzmann AOB. The stiffness parameter of the elastic model (k) is also estimated on-line by a Kalman filter and the AOB is updated in real time.

1) Different stiffness initial condition: to test the robustness of both controllers, experiments with different initial parameters were performed. In Fig.8 one can see the results for three different initial conditions.

- Condition (a): $\beta = 190$, $\alpha = 27.2$, $\gamma = 0.0345$ in Kelvin Boltzmann model and $k = 190$ in elastic model
- Condition (b): $\beta = 95$, $\alpha = 13.6$, $\gamma = 0.017$ in Kelvin Boltzmann model and $k = 95$ in elastic model
- Condition (c): $\beta = 47.5$, $\alpha = 6.8$, $\gamma = 0.006$ in Kelvin Boltzmann model and $k = 47.5$ in elastic model

In the experiment where the initial parameters were equal to the one previously estimated, the performance of both controller were similar. In the worst case, where the initials conditions are 25% of the off-line estimated parameters, the elastic controller had an unstable behavior, while the controller based on the Kelvin Boltzmann model had a small

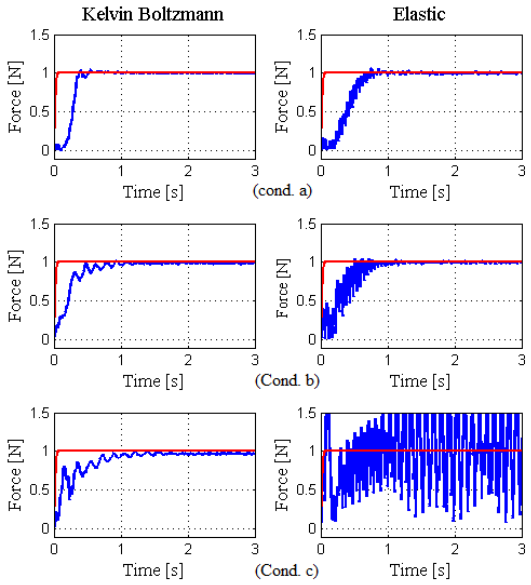

Fig. 8. Measured force in surface contact experiment with different initial conditions

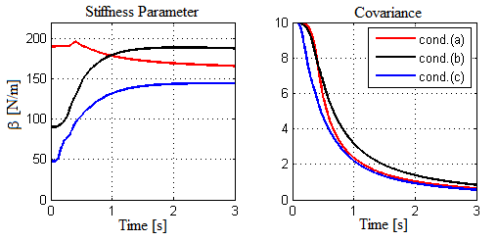

Fig. 9. Kelvin Boltzmann model: Estimated stiffness and its covariance

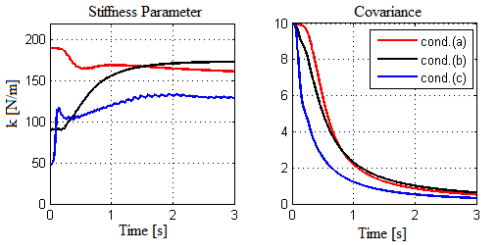

Fig. 10. Elastic model: Estimated stiffness and its covariance

vibration but kept the stability. The estimated parameters for all cases can be seen in Fig.9 and Fig.10, the values do not converge for the exactly same value in all experiments due the tissue nonhomogenity. Even though, the Kelvin Boltzmann based controller shows to be stable in all cases.

These results indicate that using a viscoelastic model one can design a more robust controller under different initial conditions.

2) Different desired closed loop poles: to evaluate the performance of both controllers with different time responses, experiments with different desired closed loop poles values were performed. The results can be seen in Fig.11.

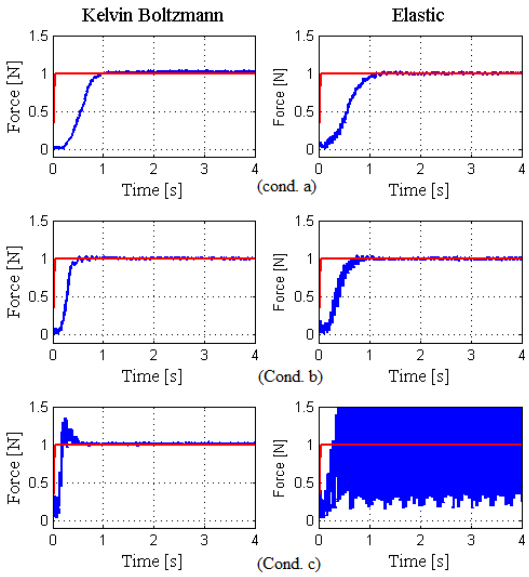

Fig. 11. Measured force in surface contact experiment with different closed loop poles. In order, all poles of the system were allocated in: $s = -10$, $s = -14$ and $s = -21$.

In Fig.11 we observe that when slow poles are set, the behavior of both controller are almost the same. This happens, for instance, when the poles are equal to -10 and the rise time for both controllers are $\tau_r = 0.8s$. The conclusion will be different in the last experiment, when the poles were set to be equal to -21. In that case the Kelvin Boltzmann controller remains stable with a rise time $\tau_r = 0.072s$ and the elastic controller even with a smaller desired raise time $\tau_r = 0.182s$ shows an unstable behavior.

With these experimental results, one can observe that using the Kelvin Boltzmann model makes possible to design controllers with a much faster time response, which is very important in cases where medical procedure deals with high velocities or high accelerations.

V. Conclusion

This paper presents the work of a force control design using an Active Observer based on viscoelastic interaction model. To the best of our knowledge, this is the first attempt to perform robot adaptive force control with Active Observers based on a realistic biological tissue interaction model. The viscoelastic model was identified and evaluated through *in vitro* relaxation experiments, and the Kelvin Boltzmann model was selected to be used in the controller design.

A control scheme using the Kelvin Boltzmann model was developed and its stability and robustness under parameters mismatches were analyzed theoretically. Experiments were performed in order to evaluate the performance of the control scheme. The experimental results show that using the Kelvin Boltzmann model one can design controllers with faster time response and more robust when compared to the same scheme in the same setup but using a purely elastic model.

This result is very helpful and indicate that the use of AOB in motion compensation tasks can be improved using the Kelvin Boltzmann model, specially when the motion disturbance has high accelerations, such as beating heart surgeries. Further work will concern experiments with more complex estimation of soft tissue parameters and experiments with physiological motion compensation. It is also planned to carry out *in vivo* experiments to test its feasibility.

References

[1] H. Paul, W. Bargar, B. Mittelstadt, B. Musits, R. Taylor, P. Kazanzides, and e. al., "Development of a Surgical Robot for Cementless Total Hip Arthroplasty", *Clinical Orthopaedics and Related Research*, vol. 285-, pp. 57-66, Dec 1992

[2] S. Bhasin, K. Dupree, P. M. Patre, and W. E. Dixon, "Neural Network Control of a Robot Interacting with an Uncertain Hunt-Crossley Viscoelastic Environment", *ASME Dynamic Systems and Control Conference*, Ann Arbor, Michigan, 2008

[3] S. G. Yuen, D. T. Kettler, P. M. Novotny, R. D. Plowes and R. D. Howe, Robotic motion compensation for beating heart intracardiac surgery, *Int. J. Robot. Res.*, vol. 28, no. 10, pp. 1355-1372, 2009.

[4] R. Cortesão, "On Kalman Active Observers" *Journal of Intelligent and Robotic Systems*, vol 48, Issue 2, February, 2007

[5] B. Cagneau, N. Zemiti, D. Bellot and G. Morel, "Physiological Motion compensation in robotized surgery using force feedback control", *Proc. IEEE Int. Conf. on Robotic and Automation*,2007, pp 1881-1886.

[6] M. Dominici, R. Cortesão and C. Souza, "Heart Motion Compensation for Robotic-Assisted Surgery: Predictive Approach vs Active Observer", *Int. Conf. on Robotic and Automation*, 2011, pp 6252 - 6257.

[7] Y. C. Fung, *Biomechanics: Mechanical Properties of Living Tissue*, Springer, 2nd Ed.; 1993.

[8] L.Barbé, B.Bayle and M. de Mathelin, "In Vivo Model Estimation and Hapatic Chacterization of Needle Insertions", *The Int. Journal of Robotics Research*, vol. 26, 2007, pp 1283-1301.

[9] M. Mahvash and P. E. Dupont, "Fast Needle Insertion to Minimize Tissue Deformation and Damage", *in IEEE Int. Conf. on Robotics and Automation*, 2009, pp. 3097-3102.

[10] A. Asadian and M. R. Kermani and R. V. Patel, "A Compact Dynamic Force Model for Needle-Tissue Interaction", *in 32nd Annual Int. Conf. of the IEEE EMBS*, 2010, pp 2292-2295.

[11] Y. Kobayashi, A. Onishi, H. Watanabe, T. Hoshi, K. Kawamura and M. G. Fujie, "In vitro Validation of Viscoelastic and Nonlinear Physical Model of Liver for Needle Insertion Simulation", *Int. Conf. on Biomedical Robotics and Biomachatronics*, 2008, pp 469-476.

[12] A. M. Okamura, C. Simone and M.D.O'Leary, "Force Modeling for Needle Insertion Into Soft Tissue", *Trans. on Biomedical Engeneering*, No 10, vol. 51 ,2004, pp 1707-1716.

[13] S. P. DiMaio and S. E. Salcudean, "Needle Insertion Modeling and Simulation", *Trans. on Robotics and Automation*, No 5, vol. 19 ,2003, pp 864-875.

[14] Y. Liu, A.E. Kerdok, and R.D. Howe, "A Nonlinear Finite Element Model of Soft Tissue Indentation",*in Proc. ISMS*, 2004, pp 67-76.

[15] R. Cortesão and P. Poignet, "Motion Compensation for Robotic-Assisted Surgery with Force Feedback", *in IEEE Int. Conf. on Robotics and Automation*, 2009, pp 3464-3469.

[16] R. Cortesão, W. Zarrad, P. Poignet, O. Company and E. Dombre, "Haptic Control Design for Robotic-Assisted Minimally Invasive Surgery", *in Int. Conf. on Intelligent Robots and Systems*, 2006, pp 454-459.

[17] W. Zarrad, P. Poignet, R. Cortesão and O. Company, "Towards Teleoperated Needle Insertion with Haptic Feedback Controller", *in Int. Conf. on Intelligent Robots and Systems*, 2007.

[18] L. Sciavicco and B. Siciliano, *Modeling and Control of Robot Manipulators* Springer, 2000.

[19] K. Ogata, *Modern Control Engineering*, Prentice Hall, 4nd Ed.; 2002.

[20] R. Cortesão, "Kalman Techniques for Intelligent Control Systems: Theory and Robotic Experiments", PhD Thesis, University of Coimbra, Coimbra, Portugal,2002.